J. exp. Biol. ***191****, 257–282 (1994)*
Printed in Great Britain © The Company of Biologists Limited 1994

IMPLICATIONS OF GILL ARCH MOVEMENTS FOR FILTER-FEEDING: AN X-RAY CINEMATOGRAPHICAL STUDY OF FILTER-FEEDING WHITE BREAM (*BLICCA BJOERKNA*) AND COMMON BREAM (*ABRAMIS BRAMA*)

COEN VAN DEN BERG, JOS G. M. VAN DEN BOOGAART, FERDINAND A. SIBBING AND JAN W. M. OSSE

Department of Experimental Animal Morphology and Cell Biology, Agricultural University, Marijkeweg 40, 6709 PG, Wageningen, the Netherlands

Accepted 9 March 1994

Summary

Previous research shows that the reducible-channel model of filter-feeding can probably be applied to common bream, but not to white bream. According to this model, zooplankton are retained in the channels between the medial gill rakers; the mesh size of the sieve can be reduced by lowering the lateral rakers of the neighbouring gill arch into these channels. Gill arch movements may well disturb this mechanism; the depressed lateral gill rakers will move in and out of the medial channels and also shift out of their centre. We have quantified these disturbances by measuring the gill arch movements during filter-feeding in white bream and common bream, using dorsal X-ray films. In both species, the lateral rakers are long enough to bridge the gill slits. It was expected that common bream, which can reduce their channels, would have considerably less shift out of the channel centre than white bream, which cannot reduce their channels. However, the predicted shift is 40–50 % of the channel width in white bream and 75 % in common bream. A new, dynamic retention mechanism is proposed for common bream. According to this hypothesis, once a particle is trapped in a reduced channel, the channel walls release mucus and the particle becomes sticky. Hence, particles need to be retained mechanically only during part of the gulping cycle. According to the hypothesis, this is achieved by sideways rotation of the lateral rakers in combination with their tapering shape. Retention mechanisms with interdigitating rakers are expected chiefly in facultative filter-feeders, because such mechanisms are easily disturbed by gill arch movements.

Introduction

Many fish species filter-feed on zooplankton by means of suction feeding (gulping) (see Sibbing, 1991). During suction feeding, water is forced through the branchial sieve by rhythmic contraction and expansion of the head. These pumping movements result in movements of the gill arches (see Hoogenboezem *et al.* 1990). In general, filter-feeding

Key words: bream, *Blicca bjoerkna*, *Abramis brama*, retention ability, filtering rate, reducible-channel model.

fishes retain zooplankton with their branchial sieve, using a variety of prey-retention mechanisms (Rubenstein and Koehl 1977). Most of these mechanisms depend to some degree on the width of the gill slits and/or on the interaction between the gill rakers and neighbouring gill arches. Hence, gill arch movements may disturb the retention mechanism of the branchial sieve.

We studied the gill arch movements during filter-feeding of white bream (*Blicca bjoerkna*) and common bream (*Abramis brama*). Hoogenboezem *et al.* (1991) proposed the reducible-channel model of filter-feeding for common bream. According to this model (Fig. 1), zooplankton are retained in the medial channels on the gill arches. The lateral rakers from one side of each gill slit can be lowered into the centre of the medial channels on the other side of the gill slit, reducing their mesh size by at least 50 %. Both the results of zooplankton feeding experiments and the presence of abductor muscles for the lateral gill rakers corroborate the reducible-channel model for common bream (Hoogenboezem *et al.* 1993; van den Berg *et al.* 1994*a*,*b*). White bream, however, cannot reduce the mesh size of its medial channels because it does not possess lateral raker abductor muscles (van den Berg *et al.* 1994*b*). Zooplankton feeding experiments show that white bream probably retains zooplankton in unreduced channels (van den Berg *et al.* 1994*a*).

The reducible-channel mechanism of prey retention is easily disturbed by gill arch movements. The mechanism does not work if the maximal gill slit width during gulping exceeds the length of the lateral rakers (Hoogenboezem *et al.* 1990). Furthermore, gill arch movements tend to shift the lateral rakers out of the centre of the medial channels, spoiling the effect of mesh size reduction (see Fig. 3A). However, when zooplankton are trapped in unreduced channels, the mesh size of the branchial sieve should be independent of gill arch movements. Therefore, the gill arch movements of common bream (which can reduce their channels) are expected to be more limited than those of white bream (which cannot reduce their channels). Furthermore, the amplitude of gill arch movements of white bream may help to explain why, in its evolution, it has not developed a reducible-channel mechanism, like the closely related common bream.

In this paper, the effect of gill arch movements on the mesh size of reduced channels is quantified by combining the movement data with data on the morphology of the branchial sieve. Hence, the data for common bream and white bream can be compared in a relevant way. Furthermore, such data allow us to judge whether the reducible-channel mechanism is feasible, given the gill arch movements.

Measurement of the head movements of suction-feeding fish is complicated by technical and computational problems (van den Berg, 1994). Such movements have been measured with X-ray cinematography (e.g. Sibbing, 1982; Sibbing *et al.* 1986; Hoogenboezem *et al.* 1990; Westneat, 1990; Claes and de Vree, 1991), but the data for these experiments may not be quantitatively reliable, since these authors ignored projection errors. For the present study, we used a three-dimensional method of analysis for single-view films (van den Berg, 1994). This accurate method was required for two reasons. First, the movement of the gill arches is expected to have both abduction and depression components; a two-dimensional method of analysis (ignoring projection errors) is inappropriate for such movements. Second, we are interested in small

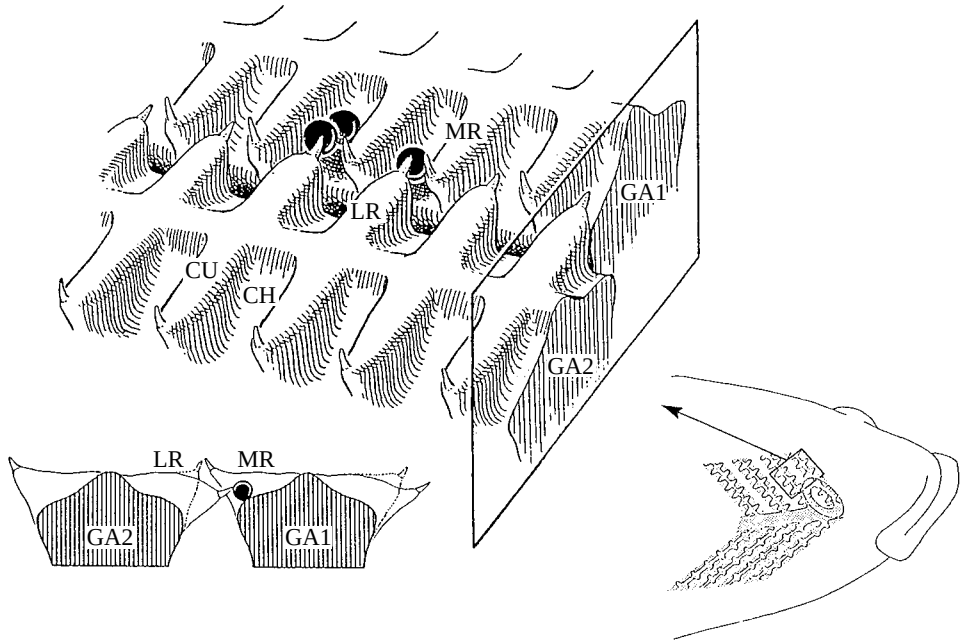

Fig. 1. These pictures illustrate the reducible-channel model of filter-feeding. The top picture shows a detail of two gill arches of the branchial sieve of common bream. The cross section indicated by the rectangle is shown in the lower left-hand picture. According to the reducible-channel model, food particles (indicated as black spheres) are retained in the medial channels of each gill arch. The channels are depressions between the raker cushions, which extend from the bony gill rakers to the middle of the gill arch surface. According to the model, the mesh size of the branchial sieve can be reduced by depressing the lateral rakers from the neighbouring gill arch into the medial channels. Adapted from Hoogenboezem *et al.* (1991). CH, channel; CU, raker cushion; GA1, GA2, gill arches 1 and 2; LR, lateral gill raker; MR, medial gill raker.

movements on the scale of individual gill rakers, hence an accuracy of at least 50 μm is required. Since we used a similar experimental design to that of Hoogenboezem *et al.* (1990), a film sequence of common bream shot by Hoogenboezem could be used. This sequence was re-analyzed with the three-dimensional method.

Materials and methods

The experimental set-up and procedures

The experimental white bream (*Blicca bjoerkna*) of 254 mm (SL) was caught in the Dutch lake IJsselmeer. It was kept in tanks of well-aerated water at 18 °C and fed with commercial food pellets and *Daphnia*, which was stored deep-frozen. For 6 months, the white bream was trained to feed freely on *Daphnia*, while living in a 14 cm×25 cm×100 cm cuvette (width×height×length). Prior to each X-ray experiment, the water level was reduced to about 11 cm, to reduce X-ray absorption by the water.

Our filming set-up consisted of a Philips Super 100 X-ray apparatus and a 9/5 inch

image intensifier in combination with an Arriflex cine camera, using 35 mm Agfa-Gevaert Scopix RP-1C film. We made dorsal X-ray films of the filter-feeding fish. The focus/image intensifier distance was 85 cm. The films were made at 60 kV, 50 frames s^{-1} with an exposure time of 5 ms, using a 1.5 mm^2 focus. During the X-ray experiments, lateral video recordings of the fish were made. The correlation between video and X-ray films was obtained using a light-emitting diode (LED) that lit up when an X-ray film sequence was being shot.

The frames of the selected film sequences were projected on sheets of paper (magnification 6.4×). The centre of each marker was indicated on the sheets. The marker positions were digitized with a Calcomp 9100 data tablet. The kinematic parameters of the movements under study were calculated using a Macintosh IIfx computer (a FORTRAN program is available on request).

An X-ray film sequence of a common bream (*Abramis brama*) (standard length, SL, 354 mm) made by Hoogenboezem *et al.* (1990) was re-analyzed with the three-dimensional method. The fish was trained and filmed under comparable circumstances to those of white bream. However, since some important markers were lacking, some parameters had to be estimated and the analysis is more restricted than that for white bream.

Platinum markers

The individual bones in the head of a feeding fish cannot be identified clearly (if at all) in X-ray films at 50 frames s^{-1}. Therefore, important positions in the fish were marked with pieces of platinum wire (diameter 0.35 mm, length 1–2 mm), which serve as identifiable points in the films. These markers were implanted surgically in the white bream, while it was anaesthetized using 100 mg l^{-1} MS 222. For details of the surgical techniques, see Hoogenboezem *et al.* (1990). As required by the three-dimensional method of analysis (van den Berg, 1994), each structure under study was marked with at least two platinum markers (Fig. 2). Several X-ray photographs were made of the marked fish to determine the real (unprojected) distances between the two markers on each structure. Using these distances and the coordinates of the projected markers on each film frame, each structure can be represented as a three-dimensional vector and the kinematic parameters (see below) can be calculated accurately (van den Berg, 1994).

Position of the markers; the kinematic parameters

Two-dimensional (qualitative) parameters

The measurements described in this paragraph can only be used as an indication of the real movement, because they are calculated with a two-dimensional method of analysis. The *mouth opening* was calculated as the distance between the projections of markers in the upper and lower lip. The *opercular expansion* was calculated as the distance between the projections of markers in each operculum. The mouth *protrusion* was calculated as the projected distance between the upper lip marker and a marker on top of the skull. The phase of these two-dimensional parameters was used as a reference for the phase of the other movements. Since opercular expansion consists primarily of abduction and

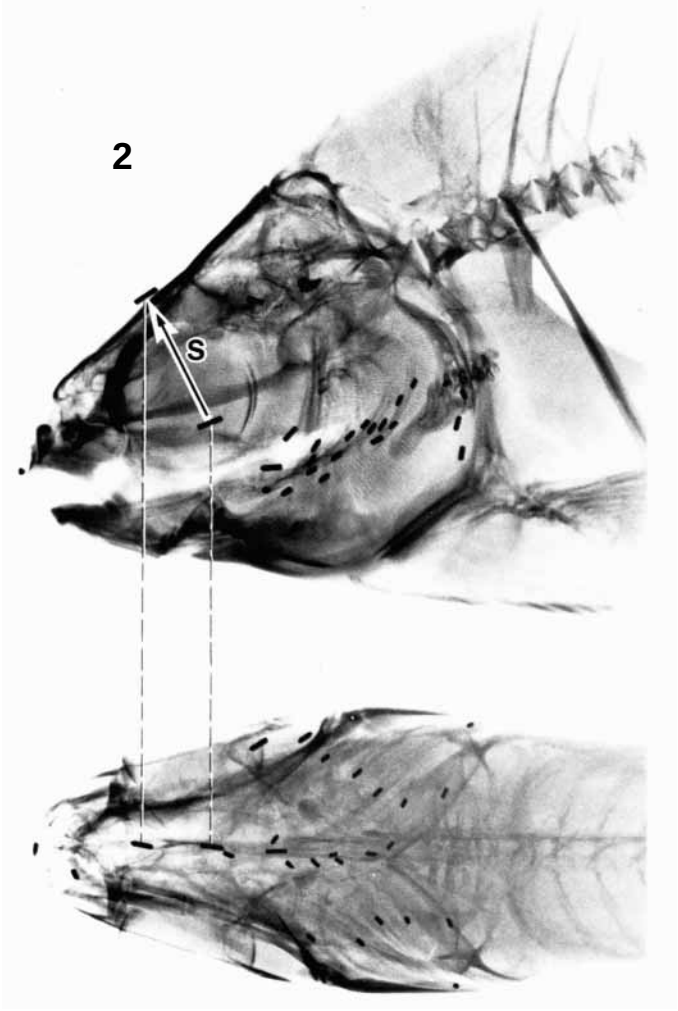

Fig. 2. Lateral and dorsal X-ray picture of the experimental white bream (SL 254 mm), showing the position of the platinum markers. A dorsal and a ventral marker on the skull surface are used to define the skull vector **S**, which is indicated in the lateral view. This vector is used to calculate depression angles in a fish-bound frame. In a similar way, each vector used in the calculations (see text) is defined by two markers.

adduction, it is largely restricted to the film plane. Therefore, the opercular expansion measurement is almost as good as a three-dimensional calculation. This does not apply to mouth opening and protrusion. A large vertical movement component is expected when the mouth is protruded. Furthermore, these measurements are influenced by the pitch of the fish.

The slit width between the first gill arch and the hyomandibula (*gill slit* 1) could not be calculated quantitatively, because these structures are not connected by a single joint. One marker was placed on the lateral side (outside) of the left hyomandibula, approximately opposite the first gill arch (the marker on the right side was rejected by the tissue of the fish prior to the experiment, a common problem in fish X-ray

cinematography). The width of the first gill slit was calculated as the perpendicular distance between the projection of the hyomandibular marker and the projection of the left first gill arch vector. This calculation is two-dimensional and hence can only be used as a rough indication of the real width of the first gill slit.

Three-dimensional (quantitative) parameters

One marker was inserted on top of the skull and one at the bottom of the skull (inside the mouth, just in front of the palatal organ). These markers define the skull vector **S** (Fig. 2). The first frame of the film sequences was defined as the reference frame, because the position of the white bream in this frame was always nearly horizontal. Skull rotation is defined as the *angle* σ between vector **S** in the reference frame and vector **S** in the subsequent film frames (van den Berg, 1994). Angle σ shows the movement of the fish skull in an earth-bound frame. It is a combination of pitch, roll and yaw. Calculation of movements in a fish-bound frame can be performed with the aid of angle σ. First, all vectors in each frame are rotated to the reference frame (using angle σ). After this transformation, movements can be calculated in a fish-bound frame (van den Berg, 1994). In the analyzed sequences, the reference vector **S** was almost perpendicular to the film plane (Fig. 2A), which is optimal for calculating parameters in a fish-bound frame (van den Berg, 1994).

The central kinematic parameter in this study is the abduction *angle* α between each gill arch and the copula communis (the fused basibranchialia which connect the gill arches mid-ventrally). Both a posterior and an anterior marker were implanted in gill arches 1–4, in the pharyngeal jaws and in the copula communis. These markers define the gill arch vectors and the copula vector. The angles α can only be calculated if each gill arch vector and the copula vector can be connected at the joint between the gill arch and the copula. It was not possible to insert platinum markers exactly above these joints; their

Fig. 3. (A) These two pictures show the medial half of the first gill arch and the lateral half of the second gill arch, each connected to the copula communis with a joint (indicated as a black circle). The spacing of the gill rakers is to scale. This diagram shows that a 10 ° adduction of the gill arches strongly affects the position of the lateral rakers with respect to the medial channels on the other side of the gill slit. The lateral rakers move deeper into the channels but also out of their centre (shift). *D*, the distance between neighbouring gill arch/copula communis joints; Med, Lat, medial and lateral sides of the gill arch; Post, Ant, posterior and anterior sides of the gill arch. (B) In this diagram of part of the branchial sieve, the positions of the markers in the gill arches and the copula communis are indicated by black oblongs. The markers in the gill arches are positioned at the lateral side (L; M, medial side). *SW* is the slit width between gill arches I and II. *W* is the width of gill arch I. (C) The marker positions are used to calculate the abduction angle α between each gill arch and the copula communis. The movement of the lateral rakers with respect to the medial channels on the neighbouring gill arch can be calculated with angle α. The relative slit width (SW_r) is the sine of angle α multiplied by the distance between the gill arch joints (*D*). The cosine of angle α multiplied by *D* indicates the shift out of the centre of the channel, or the relative raker position (*RP*). (D) When angle α_a of the anterior gill arch differs from angle α_p of the posterior gill arch, the slit width at the middle of the gill arch has to be corrected by a factor SW_c. The effect of a difference between α_a and α_p on the relative raker position (*RP*) is negligible. *L* is the length of gill arch I.

position had to be determined from a detailed X-ray photograph of the copula and the proximal part of the gill arches. In a normal X-ray photograph, the anatomical details of the copula and the gill arches are obscured by the heavy bones of the skull. Therefore, a strip of unexposed X-ray photograph was pushed into the mouth of the anaesthetized white bream (in a darkened room), placed on the copula and exposed through the ventral part of the head. In this way, the skull bones were not recorded on the X-ray photographic strip and the position of the joints relative to the implanted markers could be determined accurately. With this information, the abduction angles α could be calculated. Using angle α, two more kinematic parameters were calculated, the *slit width* (*SW*) and the *relative raker position* (*RP*) (Fig. 3B–D). A detailed description of these parameters is given in the next section.

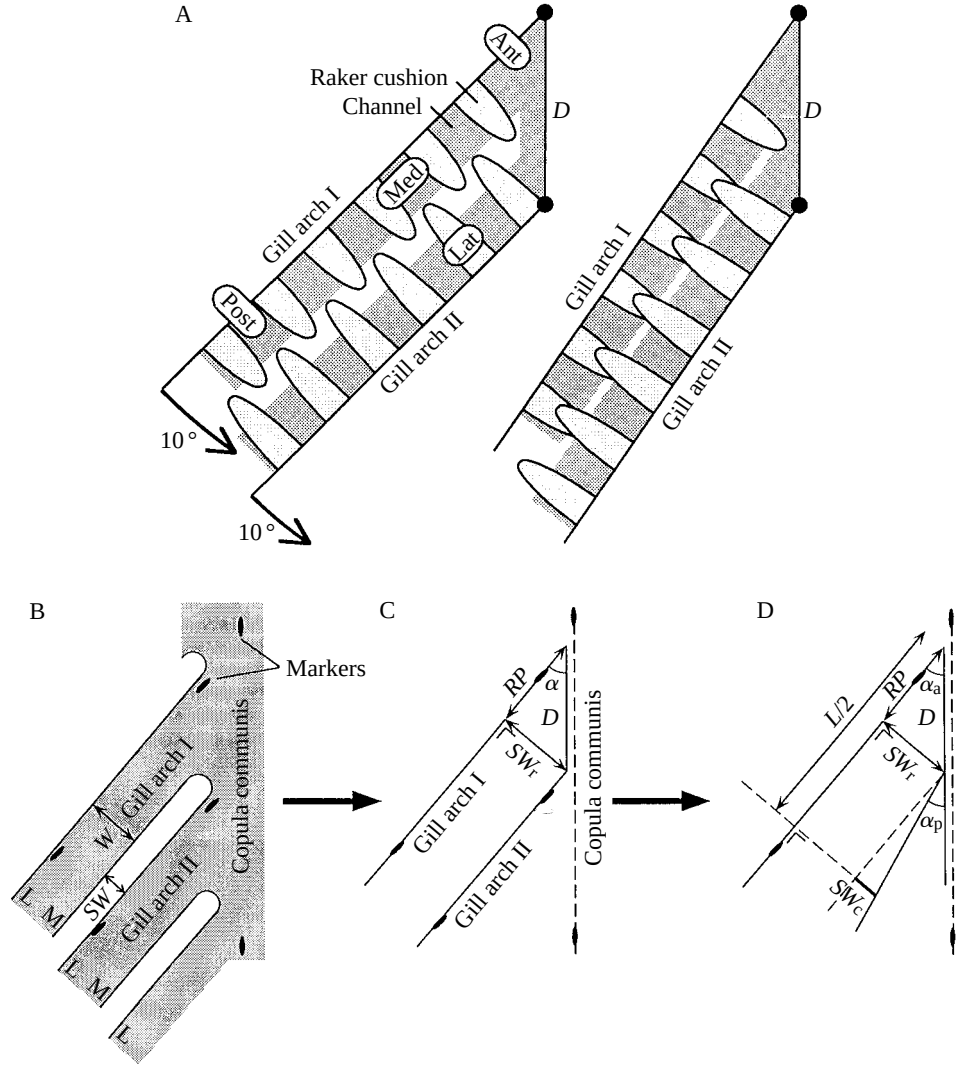

Fig. 3

The depression angles of the gill arches (*angle* β) and of the copula (*angle* γ) were calculated as well. Unlike abduction angle α, the depression angles describe the position of the branchial sieve with respect to the fish. Hence, these must be calculated in a fish-bound frame. They are defined as the angle between the gill arch/copula vector and a horizontal plane *H* in a fish-bound frame (see Fig. 5). By definition, plane *H* is parallel to the film plane in the reference frame. The angles β and γ must be calculated with the aid of the skull rotation angle σ (van den Berg, 1994).

One marker was implanted superficially in the *postlingual organ* (the muscular tissue on top of the copula communis). The movement of this marker relative to the anterior and posterior copula markers provides information about peristaltic movements of the postlingual organ (see Sibbing, 1991).

Slit width and relative raker position

As a result of the gill arch movements, the gill rakers on either side of a gill slit move with respect to each other. This movement has two components, perpendicular to and along the gill arches. It can be fully described with abduction angle α. Movements of the branchial sieve as a whole (angles β and γ) play no role. When the angles α of two neighbouring gill arches decrease, the depressed lateral rakers move deeper into the opposite medial channels and at the same time shift posteriorly, i.e. they cannot stay centred in the medial channels (Fig. 3A).

For the present detailed study of the effect of gill arch movements on filter-feeding, the relative movements of the gill rakers on either side of a gill slit must be analyzed in more detail. It is assumed that ceratobranchial 1–4 on each side lie in one plane; if this were not the case, the lateral rakers and medial channels would be out of reach. The platinum markers (Figs 2, 3B) are used to define the gill arches and the copula communis. Each gill arch position can be described with two parameters: the relative slit width (SW_r, not corrected for the width of the gill arch) and the relative raker position (*RP*) (Fig. 3B,C):

$$SW_r = D\sin\alpha\,, \tag{1}$$

$$RP = D\cos\alpha\,, \tag{2}$$

where *D* is the distance between neighbouring gill arch/copula joints

SW_r is a measure of the width of the gill slit. Furthermore, it indicates how far each depressed lateral raker is moved into the opposite medial channel. *RP* is a measure of the centring (shift) of the lateral rakers in the medial channels. *RP* is a relative measure, the exact position of the lateral rakers with respect to the medial channels is unknown.

The calculation of the real slit width is more complicated when the abduction angles α of neighbouring gill arches are unequal. When these angles are unequal, SW_r changes along the gill slit; *RP*, however, is hardly influenced (Fig. 3D). The slit width was measured at half the length (*L*) of the ceratobranchial of the anterior gill arch. Therefore, SW_r has to be corrected by adding SW_c (Fig. 3D):

$$SW_c = \tan(\alpha_a - \alpha_p)\cdot(0.5L - D\cos\alpha_a)\,, \tag{3}$$

where α_a and α_p are the angles α of the anterior and posterior gill arch respectively.

To obtain the real slit width (*SW*, Fig. 3B), the width of the gill arch has to be subtracted from the sum of SW_r and SW_c. In the experimental white bream, all gill arch markers were situated on the lateral side of the gill arches (Fig. 3B). Therefore, the width of the anterior gill arch (*W*, measured at the middle of the gill arch) was subtracted to obtain the slit width (*SW*) at the middle of the gill arch:

$$SW = SW_r + SW_c - W. \quad (4)$$

In the present X-ray films of white bream, α_a was usually slightly larger than α_p; at half the length of the gill arch, SW_c was about 5 % of SW_r. The sum of SW_r and SW_c increases along the gill arch. However, it was observed in preparations of the branchial sieves of white bream and common bream that *SW* is actually quite regular along the gill slits. The explanation is that *W* also increases along the gill arch. The increase in SW_r+SW_c is compensated for by the increase in *W*.

Results

First, the movements of the mouth, operculars, skull and postlingual organ during breathing and gulping of the white bream are treated as a general context of the movements of its branchial sieve, followed by the movements of the sieve itself. Next, the available data for common bream are presented with some comments on their accuracy. Finally, the implications of the gill arch movements for the reducible-channel model of filter-feeding are discussed.

White bream

Two film sequences of white bream filter-feeding on *Daphnia* were analyzed. Both sequences consisted of two breathing strokes followed by four gulps (checked with the synchronous video recordings).

General kinematic parameters of head movement

The general kinematic parameters are shown in Fig. 4. The peaks of the opercular expansion are indicated with vertical lines. For comparison, these lines are also drawn in Fig. 5.

In both film sequences, the frequency of the breathing strokes was roughly half that of the gulps (Table 1). Furthermore, the amplitudes of mouth opening and opercular expansion were much higher during gulping than during breathing (Fig. 4). The phase difference between mouth opening and opercular expansion during gulping was approximately 40 ms, or 12 % of the gulp cycle (Fig. 4). The second and third gulps of sequence 2 are followed by a second expansion of the operculars, but not by a clear mouth opening or protrusion.

Angle σ (skull rotation) increased to 9 ° in sequence 1 and to 16 ° in sequence 2 (Fig. 4). In the synchronous video recordings, we observed that the skull rotation consisted mainly of pitch. When angle σ increased, the snout of the fish turned down (pitch). A peak of angle σ preceded each mouth opening by approximately 40 % of a gulp cycle. In other words, prior to each gulp, the white bream turned down towards the zooplankton on the floor of the cuvette.

Table 1. *The frequency of breathing strokes and gulps and the approximate range of movements of the branchial sieve (±0.5 °) during breathing and during gulping on* Daphnia

	Sequence 1		Sequence 2		
White bream	Breathing	Gulping	Breathing	First gulp	Last gulp
Frequency (Hz)	1.7	3.5	1.7	2.5	
Range of angle α (degrees)	40–42	41–46	38–41	40–47	
Range of angle β (degrees)	24–27	32–42	22–24	24–38	21–32
Range of angle γ (degrees)	29–33	33–43	29–31	30–41	28–37

The marker in the postlingual organ moved over approximately 1.1 mm. Its forward movements were roughly synchronous with the gulps.

Although the data for the width of the first gill slit (SW_1, between the ceratobranchial of the first gill arch and the hyomandibula) result from a two-dimensional analysis, they can be compared roughly with those of the other gill slits. ΔSW_1 was 2–2.5 mm in the white bream and 4–4.5 mm in the common bream, which is almost three times larger than ΔSW_2. The peaks of SW_1 generally just preceded the peaks of opercular expansion.

Movement of the branchial sieve

The amplitude of the angles α, β and γ were always much higher during gulping then during breathing, just like the amplitudes of the opercular expansion and mouth opening (Figs 4, 5). The peaks of angle α, β and γ slightly preceded or coincided with those of the opercular expansion (Fig. 5). However, during the two secondary opercular expansions in sequence 2 (Fig. 4), the peaks of these angles followed those of the opercular expansion. This reversed phase of the opercular and branchial sieve movements suggests that the secondary peaks represent back-washing (Sibbing *et al.* 1986) (see Discussion).

The variation of abduction angle α of the left first gill arch of the white bream was almost the same in both film sequences (Fig. 5, Table 1). The depression angles β and γ (in a fish-bound frame) were different in each sequence. In sequence 1, these angles shifted to an increased level during gulping, whereas in sequence 2 they decreased slowly during gulping (Fig. 5, Table 1). In other words, during gulping the branchial sieve was slightly depressed in sequence 1, whereas it was slightly elevated, towards the palatal organ, in sequence 2.

Fig. 4. Movement of the mouth and operculae and skull rotation in two film sequences of white bream gulping on *Daphnia*. Measurements were made every 20 ms (i.e. in each frame); for clarity, the data points are connected by lines. Both film sequences show two breathing strokes followed by four gulps. The thin vertical lines indicate the peaks of opercular expansion. Note the transition from slow, low-amplitude breathing movements to fast, high-amplitude gulping movements. Note further that, in sequence 2, the second and third gulps are followed by a secondary opercular expansion. The scale in mm (left-hand *y*-axis) is placed in parentheses, because the data for opercular expansion, mouth opening and protrusion may contain projection errors. The absolute value of these data should therefore be treated with caution. Mouth opening is expected to have particularly large projection errors; hence, it is placed in parentheses.

Common bream

A film sequence of a filter-feeding common bream (Hoogenboezem *et al.* 1990) was re-analyzed with the three-dimensional method of analysis. Fig. 6 shows the mouth opening, opercular expansion and gill arch abduction angle α. The skull rotation and the

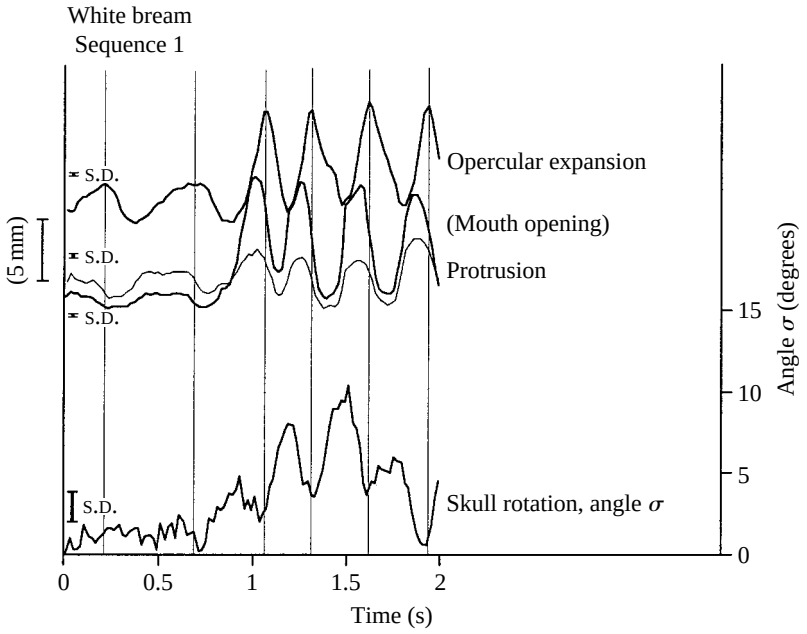

Fig. 4

depression angles could not be measured accurately. The film sequence consists of three gulps. The gulping frequency was approximately 1.2 Hz and the phase difference between mouth opening and opercular expansion was approximately 90 ms, or 11 % of the gulping cycle. The variation of angle α was larger than in the white bream: 37–46 ˚.

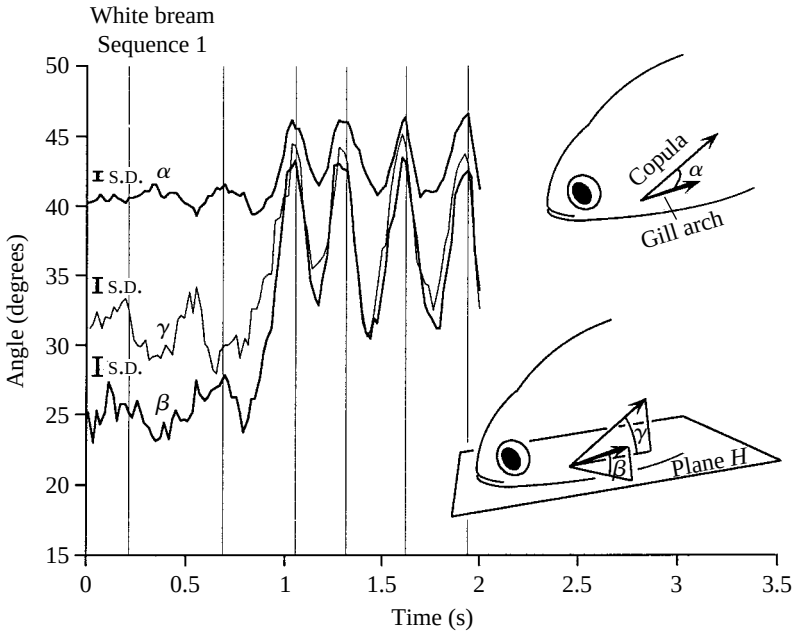

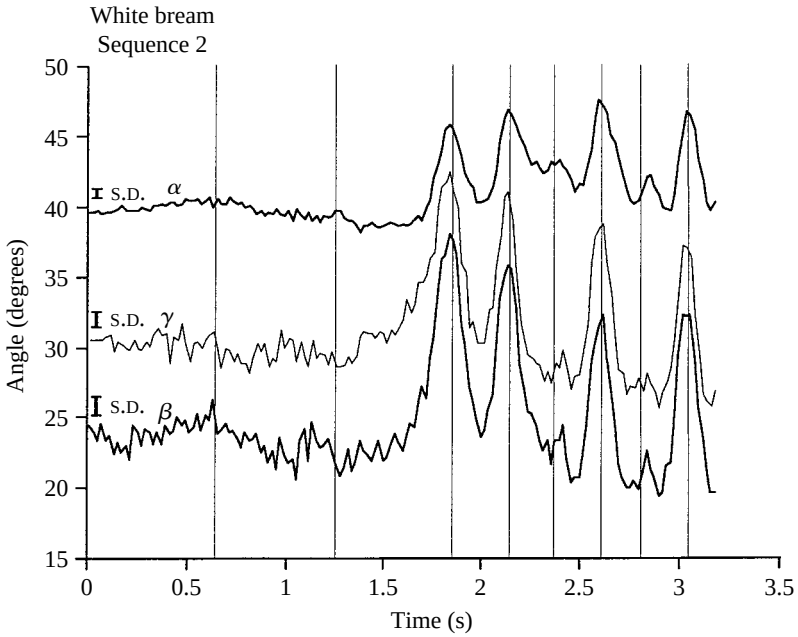

Fig. 5

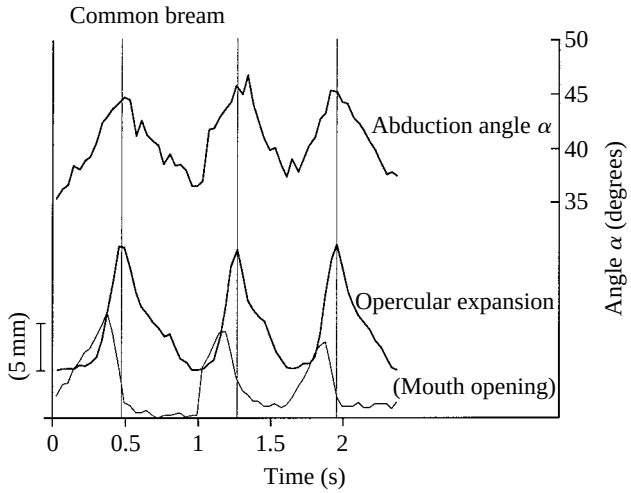

Fig. 6. This film sequence of common bream gulping on *Daphnia* from Hoogenboezem *et al.* (1990) was re-analyzed using the three-dimensional method of analysis. Measurements were made every 40 ms (i.e. in each frame); for clarity, the data points are connected by lines. The sequence shows three gulps. The thin vertical lines indicate the peaks of the opercular expansion. The scale in mm (left-hand *y*-axis) is placed in parentheses, because the data for opercular expansion and mouth opening may contain projection errors. The absolute value of these data should hence be treated with caution. Mouth opening is expected to have particularly large projection errors, hence it is put between parentheses. α, abduction angle between the left first gill arch and the copula communis.

The peaks of angle α coincided with or came slightly after the peaks of opercular expansion. The systematic error in angle α might be quite large, because some structural parameters were estimated instead of measured. These parameters are the position of the gill arch joints with respect to the markers and the distance between the gill arch joints (distance D in equations 1 and 2).

Table 2 shows the difference between the present data for the gill slit width (ΔSW) and the data of Hoogenboezem *et al.* (1990), who found an unexpected decline in ΔSW from gill slits 2–4, which we did not find. The differences between the old and new data (Table 2) are mainly caused by Hoogenboezem's two-dimensional method of analysis, but also by our rough estimation of the position of the gill arch joints. ΔSW of the second gill slit is approximately the largest (and almost the same) in both approaches. Obviously,

Fig. 5. (opposite) The rotational movements of the left first gill arch and the copula communis of white bream during film sequences 1 and 2 (compare Fig. 4). Again, the thin vertical lines show the peaks of the opercular expansion (see Fig. 4). The amplitudes of angles α, β and γ increase strongly during gulping, just like the opercular expansion and mouth movements (Fig. 4). The peaks of these angles generally precede the peaks of opercular expansion. However, during the two secondary opercular expansions in sequence 2 (Fig. 4), the small secondary peaks of angles α, β and γ come slightly after the peaks of opercular expansion. α, abduction angle between the left first gill arch and the copula communis. β, depression angle between the left first gill arch and a horizontal plane H in a fish-bound frame. γ, depression angle between the copula communis and plane H.

Table 2. *A comparison of the measurements by Hoogenboezem* et al. *(1990) with the present measurements of the variation of the slit width (*ΔSW*) in a film sequence of common bream feeding on* Daphnia

	Old results	New results
Δ*SW* 2 (mm)	1.58	1.40
Δ*SW* 3 (mm)	0.92	1.51
Δ*SW* 4 (mm)	0.43	1.62

The maximum variation (between the tips of the standard deviations) is indicated.

the largest Δ*SW* and Δ*RP* will cause the largest problems with the reducible-channel model. Hence, the three-dimensional data for this gill slit were examined in detail in white bream and common bream.

Slit width and relative raker position

During breathing, the gill slits of white bream are narrow, varying between 0 and 0.3 mm. During gulping, the amplitude of the movements is increased. As shown above, the gill arch movements can be split into the slit width (*SW*) and the relative raker position (*RP*). *SW* represents the movement of the lateral rakers in and out of the medial channels, and *RP* represents the shift of the lateral rakers with respect to the medial channels (Fig. 3A). The consequences for the reducible-channel model are best demonstrated by expressing *SW* as a fraction of the lateral raker length (*LR*) and *RP* as a fraction of the medial channel width (*CW*) (Fig. 7). Values of *CW* are 0.88 and 1.56 mm and of *LR* are 1.23 and 2.67 mm for the white and common bream, respectively (van den Berg *et al.* 1992). In both species, the maximum *SW* was approximately 60 % of *LR*. Δ*RP* was 40–50 % of *CW* for the white bream and 75 % of *CW* for the common bream (Fig. 7); the movement of the lateral rakers is markedly eccentric in both species.

Discussion

Filtering rate

The product of the frequency and amplitude of the opercular expansion can be used for a rough comparison of the flow rates of the water during breathing and gulping. It was

Fig. 7. Using the data of the abduction angle α of the left first gill arch (Figs 5 and 6), the gill slit width (*SW*) and the relative raker position (*RP*) of the second gill slit were calculated (see text). In these graphs, *SW* is plotted *versus RP* for film sequences 1 and 2 of white bream and for the sequence of common bream. Each point represents the data from one film frame. *SW* is expressed as a fraction of the lateral raker length (*LR*), and *RP* as a fraction of the medial channel width (*CW*). *SW* can be interpreted as the movement of the depressed lateral rakers in and out of the medial channels and *RP* as the shift of the lateral rakers out of the centre of the medial channels (Fig. 3A). Hence, these plots represent the total movement of the depressed lateral rakers with respect to the medial channels (compare Fig. 9). Note that these figures allow a relevant comparison of the gill arch movements of the two species, but that white bream *cannot* depress its lateral rakers. For clarity, the data for *SW* and *RP* during breathing were omitted in the plots of white bream. The standard deviations (S.D.) were estimated in one representative frame.

argued that the opercular expansion data are a good estimate of the real expansion, even though they were calculated using a two-dimensional method. It was estimated (Fig. 4) that the amplitude of the opercular expansion was three times larger during gulping than during breathing. In sequence 1, the frequency was 1.7 Hz during breathing and 3.5 Hz during gulping. Hence, the flow rate was roughly $(3.5/1.7)\times 3 \approx 6$ times larger during gulping than during breathing. During gulping, a high flow rate (=filtering rate) is

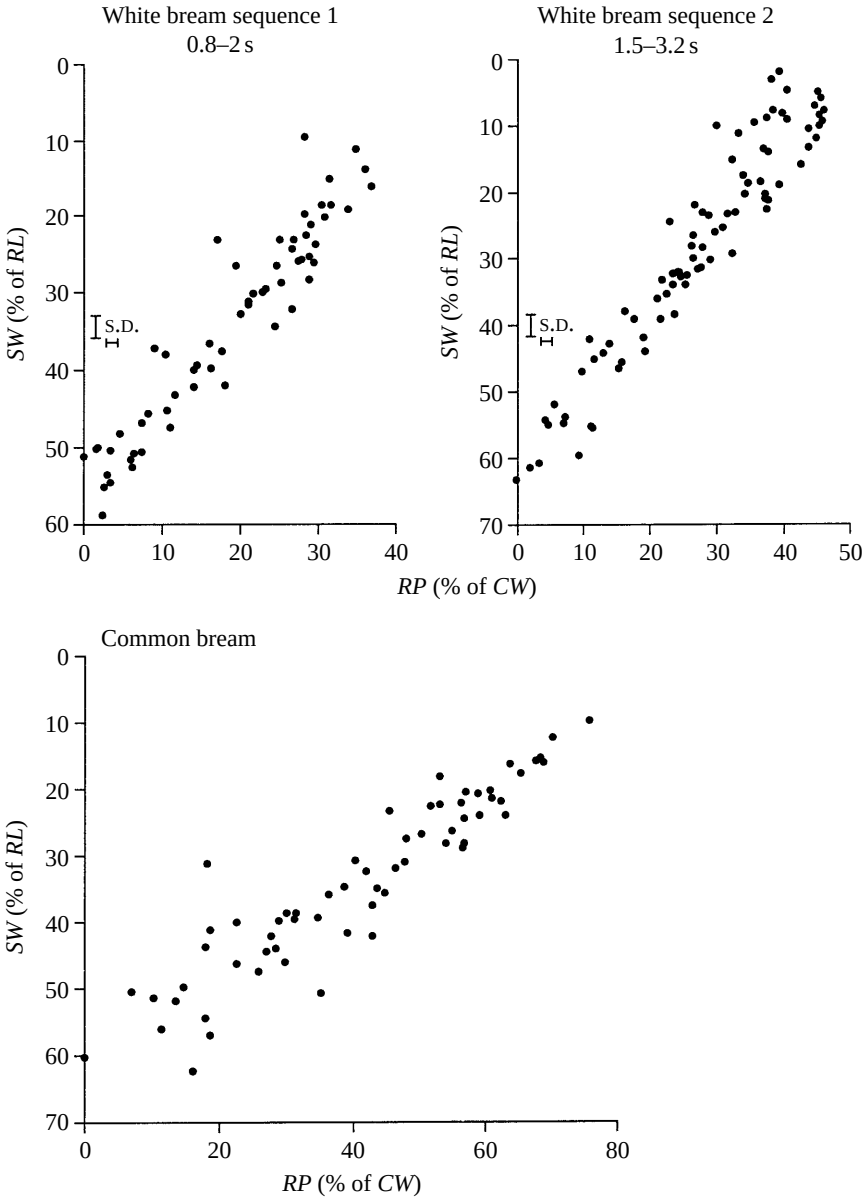

Fig. 7

advantageous because more prey are ingested per unit time. However, during gulping, the gill arch movements are larger than during breathing. What price is paid for increasing the filtering rate? Is the retention ability reduced?

Retention ability versus *gill arch movements*

Variation of the gill slit width

When the lateral rakers are depressed into the medial channels, they are not horizontal. From the realistic drawing of a cross section of a reduced channel of common bream (Fig. 1), it was estimated that their maximal depression angle is approximately 45°. Hence, the lateral rakers can bridge a gap of cos45° times the raker length, giving approximately 71 % of the raker length. The maximal slit width (*SW*) was approximately 60 % of the lateral raker length in both species (Fig. 7). Therefore, the lateral rakers of both species can *potentially* reach across the maximal gill slit width during gulping. It is important to note that white bream *cannot* depress its lateral rakers (see Introduction). However, by comparing white bream and common bream, we can judge whether the gill arch movements of common bream are adapted to keep the medial channels properly reduced.

Shift of the depressed lateral rakers in the medial channels

The shift (ΔRP) was 40–50 % of the medial channel width in the white bream and 75 % in the common bream (Fig. 7). Hence, depressed lateral gill rakers will not remain centred in the medial channels during gulping (Fig. 3A). This shift should be no problem for white bream, since it does not depress its lateral rakers into its medial channels. However, both zooplankton feeding experiments and micro-anatomical study suggest strongly that the common bream *does* reduce its medial channels when small zooplankters are abundant (Hoogenboezem *et al.* 1993; van den Berg *et al.* 1994*a*,*b*). Clearly, our previous static description of the reducible-channel model of filter-feeding in common bream has to be replaced by a dynamic one.

According to the reducible-channel model, particles are retained in a reduced channel when they get stuck between the depressed lateral raker and the walls of the medial channel. On the basis of convincing histological data for common bream, Hoogenboezem and van den Boogaart (1993) proposed the following mechanism for mucus encapsulation of trapped particles. Upon contact with the particle, the mucus cells in the medial channel walls immediately release their store of mucus. The mucus encapsulates the particle which, as a result, becomes sticky. If this hypothesis is correct, mechanical retention of the particle by the lateral raker is not required during the entire gulping cycle (Fig. 8). Probably, the particles will reach the branchial sieve in the second half of the expansion phase of the head during a gulp (between $SW_{max}/2$ and SW_{max}). According to the mechanism of Hoogenboezem and van den Boogaart (1993), the trapped particles will rapidly become sticky, i.e. during the first half of the compression phase of the head (between SW_{max} and $SW_{max}/2$). If the above assumptions are correct, the particles only need to be retained by the lateral raker during one half of the gulping cycle, from $SW_{max}/2$ to SW_{max} and back to $SW_{max}/2$, i.e. when $SW > SW_{max}/2$. When $SW < SW_{max}/2$, the trapped

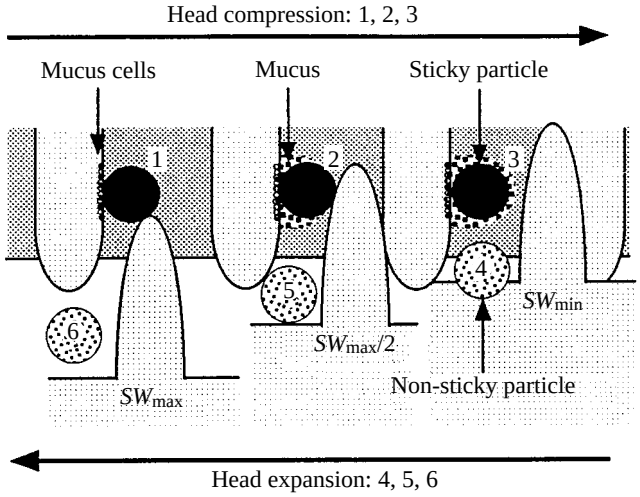

Fig. 8. This scheme illustrates the hypothetical role of mucus in the prey-retention mechanism of common bream. The medial channels of the first gill arch are drawn as being stationary. Three segments of the second gill arch show the position of the depressed lateral rakers with respect to the medial channels during maximal gill arch abduction, half-maximal abduction and maximal adduction. According to the mucus hypothesis, particles that are trapped in a reduced channel mechanically stimulate mucus secretion of the mucus cells in the channel walls. Hence, the trapped particles rapidly become encapsulated in a mucus layer (phases 1 and 2). They then stick to the channel wall and retention by the lateral rakers is no longer necessary (phase 3). It is further assumed that the particles reach the channels and become encapsulated during the second half of the expansion phase and the first half of the compression phase of each gulp. Retention of particles by the lateral rakers is only required during this part of the gulping cycle. Particles that are not properly encapsulated in mucus during the first half of the compression phase will be lost during the expansion phase of the next gulp (phases 4, 5 and 6).

particles will have become sticky. Two mechanisms may help to keep the lateral rakers centred when $SW > SW_{max}/2$. These mechanisms are described below. Next, a new, dynamic description of the reducible-channel model is given, which combines the mucus encapsulation hypothesis and both these mechanisms.

As a result of their tapering shape, the lateral gill rakers can still block the centre of the medial channels when they are not exactly centred. Hence, prey particles of half the size of the medial channel width can still be retained. In Fig. 9, the raker positions at SW_{max} and at $SW_{max}/2$ are drawn for both white bream and common bream. Note that white bream cannot depress its rakers; the figure is meant to allow a relevant comparison of the gill arch movements of both species. The lateral rakers can almost block the centres of the medial channels during this half of the gulping cycle. However, during the other half of the cycle ($SW < SW_{max}/2$), the depressed lateral rakers will collide with the medial channel walls (Fig. 9).

The lateral rakers of common bream are depressed by an abductor muscle, m. abductor branchiospinalis (Hoogenboezem *et al.* 1991). The fibres of this muscle fan out from the muscle insertion on the foot of the lateral gill raker to the muscle origin on the forked feet

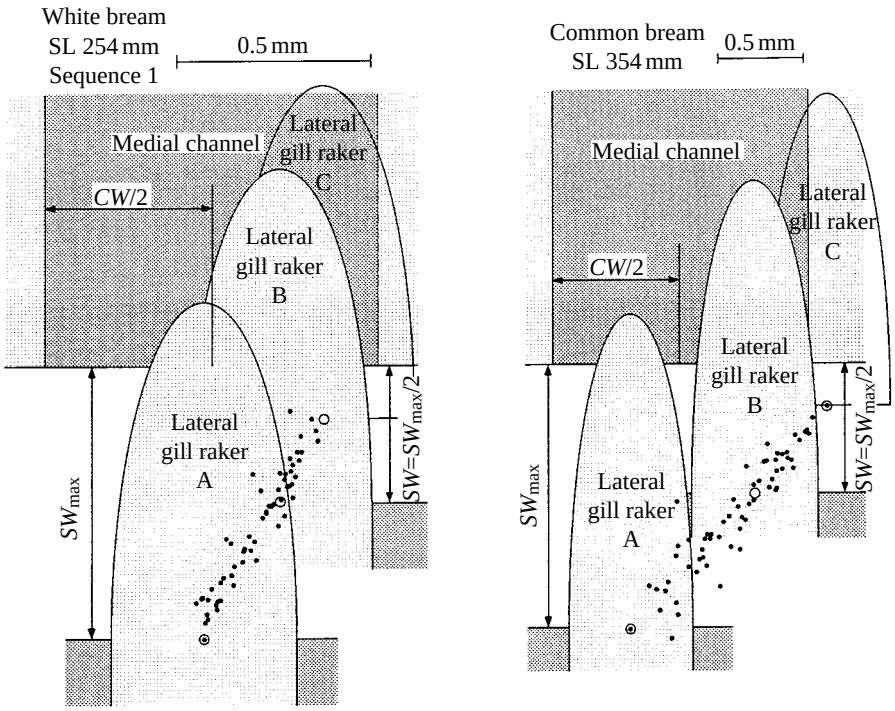

Fig. 9. Reconstruction of three positions (A, B, C) of a depressed lateral raker with respect to a medial channel during gulping. The picture of white bream was drawn for comparison with common bream; in fact, white bream *cannot* depress its lateral rakers. These pictures combine data for gill raker and channel dimensions with the data for lateral raker movement (Fig. 7). The data points of Fig. 7 are shown together with scale drawings of the gill rakers and channels. The open circles indicate the base of the lateral raker at positions A, B and C. The slit width is maximal in position A (SW_{max}). In position B, the slit width is half of SW_{max} and in position C it is minimal. These reconstructions illustrate the dynamic character of the reduced channels during gulping. The centre of the medial channels may remain blocked despite lateral raker movement: while a lateral raker moves into the opposite medial channel, its shift out of the centre of this channel (ΔRP) is partly compensated by its increasing cross section at the entrance of the channel. In position B, the centre of the medial channel is still nearly blocked in common bream (in white bream it might even be completely blocked). In position C, the slit width is minimal and the lateral raker will collide with the medial channel wall (but see Fig. 10). The angle between the depressed lateral rakers of common bream and the horizontal is approximately 45 °. Hence, the raker length in this top view is drawn as 71 % of its real length.

of the radii branchiales (van den Berg, 1994*b*). Hypothetically, a lateral raker can rotate sideways (and thus remain centred) by one-sided contraction of this muscle. The angle ϕ of sideways rotation should equal arcsine($0.5\Delta RP/LR$) to keep the lateral raker tip centred during the entire gulping cycle (Fig. 10). Angle ϕ should equal approximately 12 ° in common bream (for comparison, 8 ° in white bream). This rotation should be in phase with the gulps. De Graaf (1990) showed that in carp (*Cyprinus carpio*) the gill arches and their external musculature are both innervated by the internal pretrematic branch of the

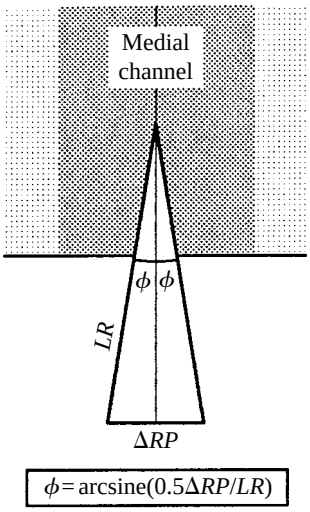

Fig. 10. This picture shows the amount of sideways rotation of a depressed lateral raker that is needed to keep its tip centred in the medial channel. The medial channel in this picture is stationary. The maximum shift (ΔRP) of the lateral raker out of the medial channel centre is shown as being symmetrical around the middle of the medial channel. At the two extreme ends of *RP*, the lateral raker should rotate over angle ϕ to keep its tip exactly centred in the medial channel. Angle ϕ can be expressed in terms of ΔRP and the raker length *LR* (see equation). Such a sideways rotation will also prevent the depressed lateral rakers from colliding with the medial channel walls when the slit width is minimal (position C in Fig. 9).

vagal ganglion. Hence, a synchronous activation of the m. abductores branchiospinales and the branchial arch muscles is not unlikely.

The above mechanisms can be combined to formulate a hypothetical, dynamic particle retention mechanism for common bream. This hypothesis is an extension of the reducible-channel model. From $SW_{max}/2$ to SW_{max} and back to $SW_{max}/2$, the particles are trapped in the reduced medial channels of the branchial sieve. During this period, they are retained mechanically by a combination of the tapering shape of the lateral rakers and sideways rotation of the lateral rakers (Figs 9, 10). The effective mesh size of the branchial sieve remains *CW*/2. Meanwhile, the particles stimulate the mucus cells in the channel walls, become encapsulated in mucus and become sticky (Fig. 8). The encapsulated particles stick to the channel walls until they are collected by back-washing; mechanical retention is not required. During maximal compression of the branchial sieve, collision of the depressed lateral rakers with the medial channel walls is prevented by active rotation of the lateral gill rakers.

According to the hypothesis above, a particle that is not properly encapsulated in mucus during the first half of the gulping cycle (e.g. because the mucus cells in the channel walls are exhausted) will be lost (Fig. 8), unless it is larger than the unreduced medial channel width. This might explain the finding in van den Berg *et al.* (1994*a*) that common bream did not retain all large particles when its medial channels were reduced.

The extended version of the reducible-channel model, as described above, can only be

applied to fish species if the structure of their branchial sieve fulfils certain requirements. (1) M. abductor branchiospinalis should be present on the lateral gill rakers of all gill arches. (2) During growth of the branchial sieve, all rakers and channels on either side of each gill slit should remain neatly interdigitated, because it is improbable that the centring of each individual lateral raker in the corresponding medial channel can be regulated separately. (3) The position of the lateral rakers with respect to the medial channels should be as in Fig. 9. As a result, during breathing the lateral rakers are expected to be directly opposite the medial rakers rather than alternating with them. (4) The maximal slit width during gulping (and hence the gulping amplitude) may not exceed a fixed value (SW_{max} in Fig. 9), which is predetermined by the structure of the branchial sieve.

Transport and collection of particles captured with the branchial sieve

In film sequence 2 of white bream, two gulps were followed by a second expansion of the operculars, but no appreciable mouth opening or protrusion (Fig. 4). The phases of the angles α, β and γ with respect to the opercular expansion were reversed (Fig. 5). This suggests that the direction of the water flow was inverted and that this movement pattern is back-washing (Sibbing *et al.* 1986). The inverted flow during back-washing probably serves to collect mucus-covered particles from the medial channels in the branchial sieve (Hoogenboezem and van den Boogaart, 1993). During back-washing, closed protrusion is expected following opercular expansion and branchial sieve movements. In the present film sequence, the closed protrusion might be hidden in the flanks of the next gulps (Fig. 4), i.e. after closed protrusion the mouth might be opened for the next gulp rather than being retracted. The X-ray films showed that the postlingual organ and the pharyngeal jaws had a reduced activity during the supposed back-washing movements, which indicates that food transport and mastication (Sibbing *et al.* 1986) did not occur.

Differences between white bream and common bream

It was shown above that gill arch movements interfere with the functioning of reduced channels. In this section, the gill arch movements of white bream and common bream are compared to investigate whether the movements of common bream are adapted for reduced channels. Next, the prey-retention mechanism of white bream is discussed, with some remarks on roach (*Rutilus rutilus*).

A fish minimizes the variation of the slit width, ΔSW ($\Delta\sin\alpha$), when angle α is in the range of 90 °; it minimizes the shift, ΔRP ($\Delta\cos\alpha$), when angle α is in the range of 0 ° (equations 1 and 2). A large ΔRP is far more serious than a large ΔSW, since ΔSW can easily be overcome by increasing the length of the lateral rakers. Therefore, it was expected that the average angle α would be smaller in common bream than in white bream. However, angle α is approximately the same in both species: on average slightly less than 45 °.

In the reducible-channel model, the palatal organ (the roof of the pharyngeal cavity) is supposed to help to guide the water flow and possibly to form the roof of the medial channels (Hoogenboezem *et al.* 1990). If the branchial sieve is strongly depressed, this becomes highly unlikely. Data from lateral X-ray films by Hoogenboezem *et al.* (1990) indicate that depression of the branchial sieve during gulping is small in common bream,

as would be expected in view of the reducible-channel model. However, the branchial sieve of the white bream was strongly depressed during gulping in our sequence 1, which is not compatible with the reducible-channel model.

The degree of expansion of the head differs drastically between breathing and gulping. Possibly, the large first gill slit width during gulping (three times larger than during breathing) serves to prevent excessive abduction of the gill arches. But how is loss of water and food particles through this slit prevented? van den Berg *et al.* (1994*b*) suggested that the lateral rakers of the first gill arch form a sieve across the wide first gill slit during gulping. The length of these rakers is approximately 1.3 mm in the white bream (SL 254 mm) and 4.4 mm in the common bream (SL 354 mm) (van den Berg *et al.* 1992). In common bream, these rakers are much longer than all other rakers. The width of the first gill slit varied by 2–2.5 mm in the white bream and by 4–4.5 mm in the common bream (two-dimensional data). Therefore, the lateral rakers of the white bream probably cannot reach across the first gill slit during the entire gulp, but those of the common bream probably can. However, the first gill slit may also be closed off by the palatal organ.

From the point of view of the reducible-channel model, the gill arch movements of common bream could be optimized by decreasing the average angle α and by decreasing the amplitude of angle α. Possibly, such changes are overruled by other demands (e.g. structural demands or the optimization of the gulp volume). Alternatively, there may have been no selective pressure on common bream to reduce the mesh size of its branchial sieve further. In contrast to the white bream, the common bream does not seem to depress its branchial sieve strongly during gulping (hence ensuring contact with the palatal organ) and it has extra long lateral gill rakers on the first gill arch, which may form a sieve across the first gill slit during gulping.

The shift (ΔRP) of white bream was smaller than that of common bream. Therefore, in white bream the centring of reduced channels would be less disturbed than in common bream. Nevertheless, both zooplankton feeding experiments and microanatomical study clearly indicate that common bream can reduce its channels and white bream cannot (van den Berg *et al.* 1994*a*,*b*). It is unclear why white bream has no m. abductores branchiospinales. The movement pattern of its gill arches is well suited for channel reduction. White bream might become a better filter-feeder than common bream just by investing in a set of tiny raker abductor muscles.

Which retention model should be used to describe the feeding of white bream on zooplankton? The maximum slit width of the white bream is almost equal to its medial channel width. According to the saw-tooth model of filter-feeding (Sibbing, 1991), the gill slits are the meshes of the sieve, which retains particles larger than the gill slit width. Therefore, one might assume that the saw-tooth model could be applied to white bream. However, a prediction of the saw-tooth model is that *Daphnia* are not retained as well as copepods, because of their flatness (van den Berg *et al.* 1993). Such a difference was not found for white bream (van den Berg *et al.* 1994*a*). Hence, the unreducible-channel model (retention in the medial channels, but no means of reducing their mesh size) is the best model for the zooplankton retention mechanism of white bream. van den Berg *et al.* (1994*a*) showed that the saw-tooth model can probably be applied to roach (*Rutilus*

rutilus). Although we did not succeed in making X-ray films of filter-feeding roach, the gill arch movements of roach that would be expected if the saw-tooth model were to apply, on the basis of the zooplankton retention data (van den Berg *et al.* 1994*a*), are comparable to those of white and common bream. In freshly killed roach, angle α is approximately 45°, just as it is in common and white bream. Hence, at present it is justified to describe zooplankton retention by roach with the saw-tooth model of filter-feeding.

The conflict between filtering rate and retention ability

The reducible-channel model induces a conflict between increasing the amplitude of the head movements (to increase the filtering rate) and reducing the medial channel width (to increase the retention ability); in other words, a conflict between number of prey taken up per unit time and minimum size of prey that can be retained.

Common bream has pushed its gill arch movements, on the one hand, and the size of its medial channels, on the other hand, to the limits allowed by the reducible-channel model. If ΔRP were more than 75 % of *CW*, rotation of the depressed lateral rakers could no longer prevent them from being pushed into the medial channel walls when *SW* is minimal. The gulping movements therefore set severe limits to the use of the reducible-channel mechanism of filter-feeding.

A fine sieve with a mesh size of 10–70 μm, as found in the silver carp (*Hypophthalmichthys molitrix*), a cyprinid obligate filter-feeder, cannot be achieved with the reducible-channel mechanism; indeed, silver carp does not use an interdigitating sieve (Smith, 1989). The reducible-channel model is typically a retention mechanism for *facultative* filter-feeders, such as common bream. The major advantage of the reducible-channel model for common bream is the adjustability of the mesh size. Zooplankton is not the only food source for common bream. Chironomid larvae are an important food source, as well. If the branchial sieve is too fine, separating food from substratum becomes difficult (Janssen, 1978). Therefore, the coarse sieve of common bream (unreduced channels) is suited to filter chironomid larvae from substratum, while the fine sieve (reduced channels) is better suited for filtering small zooplankton from the water (see van den Berg *et al.* 1994*a*).

Error analysis

Errors due to divergence of the X-ray beams

The distance to the X-ray source

The distance between the X-ray source and the image intensifier was 85 cm. The magnification (M) of a structure is dependent on its distance x (in cm) from the X-ray source, because the X-ray beam diverges: $M=85/x$. The white bream always fed from the floor of the cuvette. During a film sequence, the distance between each gill arch and the image intensifier varied between approximately 2 and 3 cm. Therefore, the magnification of each gill arch varied from approximately 1.024 to 1.037 (i.e. by 1.2 %).

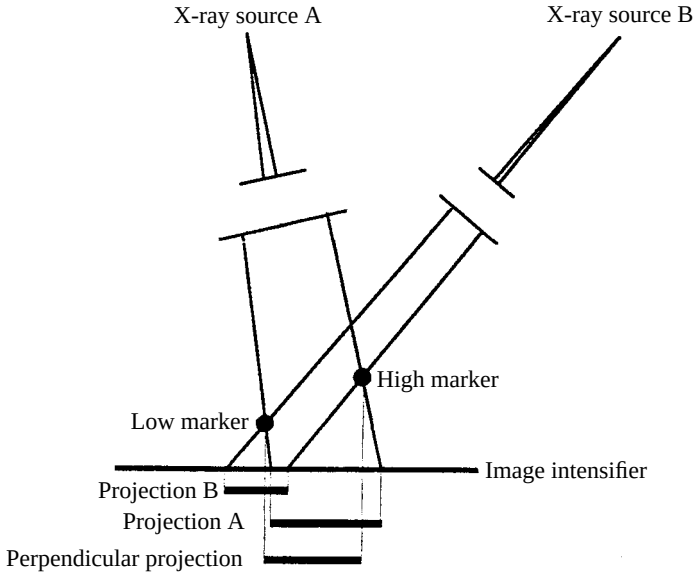

Fig. 11. Projection errors may occur when two markers have a different vertical distance from the image intensifier, as shown here. The projected distance between these markers depends on their position with respect to the X-ray source, as illustrated here for two very different positions (exaggerated) of the X-ray source (A, B) with respect to the markers.

The orientation with respect to the X-ray beams

The projected length of a structure is dependent on its orientation relative to the X-ray beam (Fig. 11). In the white bream, the vertical distance between the markers on the top and on the base of the skull was approximately 2 cm (Fig. 2). The distance between the lower marker and the image intensifier was approximately 3 cm. For realistic sideways movement of the fish in the cuvette, the magnification of the projection of the skull vector varies by some 3 %. The vertical distance between the markers in the gill arches and the copula does not exceed 1 cm. Hence, this error will be less than 1 % for the gill arch and copula vectors.

Deformation by the image intensifier

Deformation by the image intensifier was determined by Hoogenboezem *et al.* (1990) by filming a steel grid with square meshes. They found that the error increased rapidly from the centre to the edges; in a central circle of 10 cm diameter it was less than 1.6 %. During filming, the head of the white bream was always well within this area.

The lens error of the film projector

Deformation due to projection of the film frames on paper was measured by projecting paper with 1 mm squares. The error increases rapidly from the centre to the edges. It was 2–3 % at the edges and less than 1 % in the central area, where the image of the fish was always projected.

Errors in the measurement of the anatomical constants

The unprojected distance between marker pairs

An error in the measurement of the real distance between the two markers in each structure causes a systematic error in the calculations. This source of errors was tested by altering the value of these distances in the computer calculations. An error of 1 mm caused a systematic error in angle α of the first gill arch of approximately 0.7–0.8 °. Such an error would occur if the angle between the gill arch vector of 20 mm and the plane of the X-ray photograph in which the distance is measured is 18 ° instead of 0 °; in fact, the X-ray photographs were much better than that.

The position of the gill arch/copula joint

If the real position of the gill arch/copula joint is 1 mm more caudal than measured in the X-ray photographic strips, the error in angle α is approximately 0.7 ° (determined by altering parameters in the computer calculations). The calculation of angle α is clearly not very sensitive to this type of systematic error. The real error in the position of the joint is probably much less than 1 mm.

The measuring error

The measuring errors are somewhat dependent on the depression angles of the structures. We projected one representative frame ten times and calculated the standard deviations (S.D.) of the ten sets of data points. The S.D. of the angles was always (much) less than 1 °. The S.D. of *RP* and *SW* was always less than 50 μm.

List of symbols

Plane *H*	horizontal plane in a fish-bound frame; by definition plane *H* is parallel to the film plane in the reference frame of each film sequence
CW	medial channel width
D	the distance between neighbouring gill arch/copula communis joints
L	length of the ceratobranchial of the gill arch
LR	lateral gill raker length
RP	relative position of the lateral gill rakers with respect to the medial channels; centring of the lateral gill rakers
ΔRP	shift; variation of *RP*
SW	real gill slit width
ΔSW	variation of SW
SW_1, SW_2	slit widths of the first and second gill slits
SW_{max}, SW_{min}	maximal and minimal value of *SW* during gulping
SW_c	slit width factor, which corrects for the effect of $\alpha_a \neq \alpha_p$
SW_r	relative slit width (not corrected)
W	gill arch width (measured at the middle of the ceratobranchial)
α	abduction angle between a gill arch and the copula communis
α_a, α_p	angle α of the gill arch on the anterior and the posterior sides of a gill slit

β depression angle of a gill arch; the angle between a gill arch and plane H
γ depression angle of the copula communis
σ rotation angle of the skull; angle between the skull vector in a particular frame and the skull vector in the reference frame.

Two anonymous referees are acknowledged for their thorough evaluation of the manuscript. This research was supported by the Foundation for Fundamental Biological Research (BION), which is subsidized by the Netherlands Organization for Scientific Research (NWO), project number 811-428-265. The OVB (Organization for Improvement of Inland Fisheries) provided fishes for this research. Kareltje and Geert van Snik are thanked for their help in making the X-ray films.

References

CLAES, G. AND DE VREE, F. (1991). Kinematics of the pharyngeal jaws during feeding in *Oreochromis niloticus* (Pisces, Perciformes). *J. Morph.* **208**, 227–245.

DE GRAAF, P. J. F. (1990). Innervation pattern of the gill arches and gills of the carp (*Cyprinus carpio*). *J. Morph.* **206**, 71–78.

HOOGENBOEZEM, W., LAMMENS, E. H. R. R., MACGILLAVRY, P. J. AND SIBBING, F. A. (1993). Size selectivity and sieve adjustment in filter-feeding bream *Abramis brama* (L.), Cyprinidae. *Can. J. Fish. aquat. Sci.* **50**, 465–471.

HOOGENBOEZEM, W., SIBBING, F. A., OSSE, J. W. M., VAN DEN BOOGAART, J. G. M., LAMMENS, E. H. R. R. AND TERLOUW, A. (1990). X-ray measurements of gill-arch movements in filter-feeding bream, *Abramis brama* (Cyprinidae). *J. Fish Biol.* **36**, 47–58.

HOOGENBOEZEM, W. AND VAN DEN BOOGAART, J. G. M. (1993). The importance of oro-pharyngeal mucus in filter-feeding of bream (*Abramis brama*). *Can. J. Fish. aquat. Sci.* **50**, 472–479.

HOOGENBOEZEM, W., VAN DEN BOOGAART, J. G. M., SIBBING, F. A., LAMMENS, E. H. R. R., TERLOUW, A. AND OSSE, J. W. M. (1991). A new model of particle retention and branchial sieve adjustment in filter-feeding bream (*Abramis brama* (L.), Cyprinidae). *Can. J. Fish. aquat. Sci.* **48**, 7–18.

JANSSEN, J. (1978). Feeding-behavior repertoire of the alewife, *Alosa pseudoharengus*, and the ciscoes *Coregonus hoyi* and *C. artedii*. *J. Fish Res. Bd Can.* **35**, 249–253.

RUBENSTEIN, D. I. AND KOEHL, M. A. R. (1977). The mechanisms of filter feeding: some theoretical considerations. *Am. Nat.* **111**, 981–994.

SIBBING, F. A. (1982). Pharyngeal mastication and food transport in the carp (*Cyprinus carpio* L.): a cineradiographic and electromyographic study. *J. Morph.* **172**, 223–258.

SIBBING, F. A. (1991). Food capture and oral processing. In *Cyprinid Fishes; Systematics, Biology and Exploitation* (ed. I. J. Winfield and J. Nelson), pp. 377–412. London: Chapman and Hall.

SIBBING, F. A., OSSE, J. W. M. AND TERLOUW, A. (1986). Food handling in the carp (*Cyprinus carpio*): its movement patterns, mechanisms and limitations. *J. Zool., Lond.* A **210**, 161–203.

SMITH, D. W. (1989). The feeding selectivity of silver carp, *Hypophthalmichthys molitrix* Val. *J. Fish Biol.* **34**, 819–828.

VAN DEN BERG, C. (1994). A quantitative, three-dimensional method of analyzing rotational movement from single-view movies. *J. exp. Biol.* **191**, 283–290.

VAN DEN BERG, C., SIBBING, F. A., OSSE, J. W. M. AND HOOGENBOEZEM, W. (1992). Structure, development and function of the branchial sieve of common bream, *Abramis brama*, white bream, *Blicca bjoerkna*, and roach, *Rutilus rutilus*. *Envl Biol. Fish.* **33**, 105–124.

VAN DEN BERG, C., VAN DEN BOOGAART, J. G. M., SIBBING, F. A., LAMMENS, E. H. R. R. AND OSSE, J. W. M. (1993). Shape of zooplankton and retention in filter-feeding. A quantitative comparison between industrial sieves and the branchial sieves of common bream (*Abramis brama*) and white bream (*Blicca bjoerkna*). *Can. J. Fish. aquat. Sci.* **50**, 716–724.

VAN DEN BERG, C., VAN DEN BOOGAART, J. G. M., SIBBING, F. A. AND OSSE, J. W. M. (1994*a*).

Zooplankton feeding in common bream (*Abramis brama*), white bream (*Blicca bjoerkna*) and roach (*Rutilus rutilus*): experiments, models and energy intake. *Neth. J. Zool.* **44** (in press).

VAN DEN BERG, C., VAN SNIK, G., VAN DEN BOOGAART, J. G. M., SIBBING, F. A. AND OSSE, J. W. M. (1994*b*). Comparative microanatomy of the branchial sieve in three sympatric cyprinid species related to filter-feeding mechanisms. *J. Morph.* **219**, 73–87.

WESTNEAT, M. W. (1990). Feeding mechanics of teleost fishes (Labridae; Perciformes): a test of four-bar linkage models. *J. Morph.* **205**, 269–296.